PRACTICAL PAPER

Resolution Enhancement of Multispectral Image Data to Improve Classification Accuracy

Abstract

This study evaluated several methods for enhancing the spatial resolution of multispectral images using a higher resolution panchromatic image. A new method that relies on the local correlation between the low resolution superpixel and the corresponding mean panchromatic radiance is presented. High resolution multispectral images are produced based on the local correlation value and the high resolution panchromatic brightness levels. This method allows for within-pixel local adaptation of the correlation values to account for mixed pixel effects. The resultant hybrid, high resolution, multispectral data set has increased visual interpretability and improved classification accuracy while preserving the radiometric integrity of the original multispectral data. These methods can be applied to create simulated high resolution multispectral data to enhance existent image analysis techniques such as land-cover classification.

Introduction

An inevitable trade-off in the collection of electro-optical remotely sensed imagery is that between spatial and spectral resolution. Spatial resolution defines the degree of fine detail that can be seen in an image. It is dictated by the projection of the detector through the optical collection system back onto the target. Spectral resolution can be thought of as the width of the bandpass over which the incoming radiance field is measured. The finer this bandpass is, the higher the spectral resolution of the sensing system is considered (Lillesand and Kiefer, 1979).

Spatial resolution is an invaluable asset for imagery that is being used for mapping, photogrammetric measurements, or interpretation purposes. Spectral resolution provides important information for land-cover classification and spectral interpretation, as well as a host of other image analysis procedures.

With today's suite of remote sensing collection systems and conventional digitized air photo data, many systems are available with strengths in the different types of resolution mentioned. To be able to merge data from the different sensors and take advantage of the capabilities of each is an important topic. This paper reviews some procedures for merging multispectral imagery with higher resolution panchromatic scenes. An improved image merger method is then presented. The objective of the improved image merger method is to generate hybrid high resolution multispectral images that attempt to preserve the radiometric characteristics of the original multispectral data. The primary goal of this effort is to improve land-cover classification accuracy. The images resulting from the process were, therefore, evaluated on the basis of classification accuracy and were compared using an approach similar to that proposed by Price (1987).

Background

The 1980s and the early part of this decade have seen much research carried out in the field of scene merger. The availability of satellite data of varying resolution and the desire for better data has prompted many viable techniques.

Early studies reported successful merging of the Landsat Multispectral Scanner (MSS) with many other imaging modalities. Merger with both airborne and shuttle based (SIR-A) radar images have been shown by Daily *et al.* (1979) and Chavez *et al.* (1983). Lauer and Todd (1981) combine data from the Return Beam Vidicon (RBV) with that from the MSS while Schowengerdt (1982) merged Heat Capacity Mapping Mission (HCMM) data with MSS data. Since the introduction of the Landsat Thematic Mapper (TM) and the SPOT HRV (P and XS), much additional research has been carried out.

These merger techniques can be roughly placed into three categories; merger for display, merger by separate manipulation of spatial information, and merger to maintain radiometric integrity.

The mergers for display techniques have been coined by Price (1987) as the *ad hoc* approaches. These techniques are primarily concerned with enhancement of the image for an interpreter's display and are not of particular interest here.

Multispectral image data can be thought of as being composed of two components, a spatial and a spectral component. The second category of merger techniques—merger by separate manipulation of spatial information—tries to separate these components and enhance the spatial information without touching the spectral information. Chavez *et al.* (1991) has performed a comparative study of three techniques falling within this category of merger algorithms; HIS, principal components analysis (PCA), and high-pass filter (HPF) procedures. This study used statistical, visual, and graphical means of comparison between methods but mentioned nothing of the utility of the merged data for land-cover classification.

Visual enhancement is not always the aim of such merger techniques; however, it is one result from the techniques in the previous two categories. If the resulting hybrid image is to be used in automated image analysis algorithms, radiometric integrity needs to be maintained. The third category of techniques, merging to maintain radiometric integ-

Curtis K. Munechika, James S. Warnick, Carl Salvaggio, and John R. Schott

Rochester Institute of Technology, Center for Imaging Science, Digital Imaging and Remote Sensing Laboratory (DIRS), Chester F. Carlson Building, P. O. Box 9887, Rochester, NY 14623-0887

Photogrammetric Engineering & Remote Sensing,
Vol. 59, No. 1, January 1993, pp. 67–72.

0099-1112/93/5901-63$03.00/0

rity, addresses this requirement. This category is similar to the *ad hoc* techniques; however, it is more statistically rigorous in its attempt to maintain radiometric fidelity.

Pradines (1986) has proposed a method for merging four SPOT Pan pixels with a corresponding SPOT XS pixel, as illustrated in Figure 1, whereby

$$XP_J = X \cdot \frac{P_J}{P_1 + P_2 + P_3 + P_4}, \ (J = 1, \ldots, 4) \tag{1}$$

where XP_J is the resultant hybrid output pixel in the Jth position, P_J is the high resolution panchromatic digital count (DC) in the Jth position, and X is the original low resolution DC. This method results in an aggregate of four hybrid pixel with the radiometry of the original image. This technique requires that the panchromatic channel be strongly correlated with the individual multispectral bands; otherwise, the results would prove invalid.

Price (1987) has proposed a two-stage merger method. This method consists of a stage for enhancing the multispectral bands that are strongly correlated with the high resolution panchromatic image and a second stage for weakly correlated multispectral bands.

Stage 1 of Price's method proceeds under the assumption that, because the multispectral bands exhibit a strong correlation with the panchromatic data set, the relationship between the DCs from these images can be described as linear. The relationship proposed is

$$XS_i = a_i \cdot \mathrm{PAN_{ave}} + b_i \tag{2}$$

where XS_i is the DC of a superpixel (the area comprised by one low resolution multispectral pixel) in the ith multispectral band, $\mathrm{PAN_{ave}}$ is the average DC in the corresponding superpixel in the high resolution panchromatic image, and a_i and b_i are least-squares regression coefficients for the ith multispectral band. After solving for a_i and b_i, a high resolution hybrid multispectral estimate image can be formed as

$$XS_i' = a_i \cdot \mathrm{Pan_{HR}} + b_i \tag{3}$$

$$\mathrm{Hybrid}_i = \frac{XS_i \cdot XS_i'}{XS'_{(\mathrm{avg}.i)}} \tag{4}$$

for the ith multispectral band. In Equations 3 and 4, Hybrid_i is the DC in the ith high resolution hybrid multispectral band, XS'_i is the high resolution estimate of the ith XS band, and $XS'_{(\mathrm{avg}.i)}$ is the average of the DC in the XS'_i image in the corresponding XS_i superpixel. This method is similar to Pradines' method with the exception that Price uses an estimate of a multispectral band instead of the panchromatic data directly for the merging operation. Price's resulting hybrid image has a superpixel average DC that is the same as the original multispectral band while Pradines' method requires that the sum of the hybrid DCs within the superpixel equal the original multispectral value.

Price's stage 2 procedure for weakly correlated bands assumes that the relationship between the low resolution multispectral bands and the high resolution panchromatic image can not be considered linear. A look-up-table (LUT) was computed as follows. All pixels in the high resolution panchromatic image that fell within a defined superpixel were averaged, and a new image was formed at the same resolution as the low resolution multispectral image. Mean values of the DCs in the weakly correlated multispectral bands that fall in the same locations as the individual values in the averaged panchromatic image are computed (i.e., wherever there is a DC of 1 in the averaged panchromatic image, compute the average values of all the corresponding multispec-

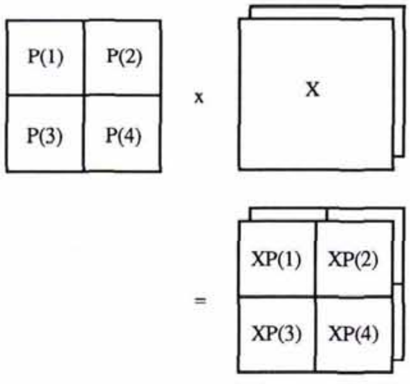

Fig. 1. Illustration of Pradines' (1986) merger method.

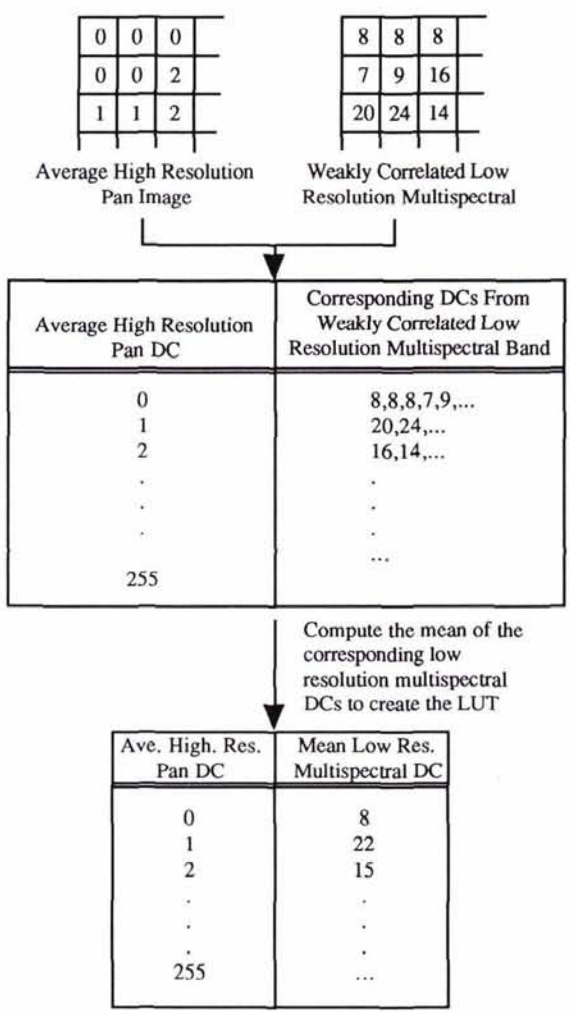

Fig. 2. Formation of the LUT used by Price (1987) to determine a high resolution multispectral estimate for weakly correlated bands.

tral DC) (see Figure 2). These data form a LUT that can be used to form a high resolution estimate of the ith multispectral band, the same as XS'_i in stage 1. The high resolution hybrid multispectral bands for these weakly correlated data are then computed in an identical manner as the strongly correlated bands (Equation 4).

Price illustrated this method using simulated SPOT 10-m panchromatic data with the three 20-m multispectral channels. Channels 1 and 2 (the green and red data) proved strongly correlated with the panchromatic data (above 99 percent) while channel 3 was weakly correlated (approximately 87 percent). Price did not test his results in terms of attainable classification accuracy, only in terms of absolute errors. Price's method will be used as a reference for comparison of the attainable classification accuracy using the new techniques presented here.

Enhancement Methods

The merger methods developed during this study fell under the third category of merger methods, merging to maintain radiometric integrity. Their applicability include only those low resolution multispectral bands that exhibit a strong correlation with the input high resolution panchromatic data.

The data sets to be merged consist of a high resolution panchromatic image (e.g., SPOT HRV PAN) and a low resolution multispectral image (e.g., Landsat TM). The low resolution multispectral image was pixel replicated to contain approximately the same number of pixels as the high resolution panchromatic image for a defined area, and was resampled with a unit convolution kernel having a size equivalent to the replication dimension to eliminate the introduced blockiness. The high resolution panchromatic image was then geometrically registered to the pixel replicated low resolution multispectral image (this preserves the original radiometric data in the multispectral image).

The method, that will be referred to as the ratio method is summarized by

$$DC_{Hybrid\ XS(i)} = DC_{Hi\ Res\ Pan} \frac{DC_{Low\ Res\ XS(i)}}{DC_{Syn\ Pan}} \tag{5}$$

where $DC_{Hybrid\ XS(i)}$ is the ith band of the output high resolution hybrid multispectral image, $DC_{Hi\ Res\ Pan}$ is the corresponding pixel in the high resolution input panchromatic image, $DC_{Low\ Res\ XS(i)}$ is the superpixel digital count in the ith band of the input low resolution multispectral image, and $DC_{Syn\ Pan}$ is the corresponding low resolution synthetic panchromatic digital count in an image created from those low resolution multispectral bands that overlap the spectral response of the input high resolution panchromatic band. This synthetic panchromatic image represents the best estimate of the input high resolution panchromatic image that can be formed from the input low resolution data. This gives a mean radiometric equivalence in Equation 5 of the two panchromatic data sets.

This synthetic panchromatic image was created using a modification to the approach described by Suits *et al.* (1988) to substitute signals from one sensor for those produced by another. Given the reflectance spectrum of a target, some atmospheric parameters, and an atmospheric model such as LOWTRAN (Kneizys *et al.*, 1988), one can estimate the radiance that reaches a sensor in a bandpass of interest. This radiance can be described as

$$L_s = \frac{\int_0^\infty L_\lambda \cdot \beta_\lambda \, d\lambda}{\int_0^\infty \beta_\lambda \, d\lambda} \tag{6}$$

where L_s is the effective radiance seen by the sensor, L_λ is the radiance reaching the sensor, and β_λ is the sensor's normalized spectral response function. The estimated digital output from the sensor was

$$DC'_i = \frac{L_{si} - \text{offset}_i}{\text{gain}_i} \tag{7}$$

where DC'_i is the sensor's output digital count corresponding to the effective radiance L_{si}, and gain_i and offset_i are the sensor's calibration coefficients for the ith spectral band. For the case of a merger involving the panchromatic band of the SPOT HRV (10-m GIFOV) and the reflective bands of Landsat TM (30-m GIFOV), the weighting factors needed to compute the synthetic panchromatic image are obtained from a multiple linear regression of the form

$$DC'_{SPOT} = \varphi_1 DC'_{TM\,1} + \varphi_2 DC'_{TM\,2} + \varphi_3 DC'_{TM\,3} + \varphi_4 DC'_{TM\,4} + \epsilon \tag{8}$$

where DC′ are the estimated digital signals from the subscripted sensors (using Equations 6 and 7), ω_i ($i = 1, 4$) are the weighting factors for the appropriate low resolution multispectral bands, and ϵ is the error to be minimized by the regression.

The synthetic panchromatic image is then formed as

$$DC_{Syn\ Pan} = \sum_{i=1}^{4} \varphi_i DC_{TM\ i} \tag{9}$$

where $DC_{TM\,i}$ are the original DC from the low resolution multispectral band i. In order to obtain all the parameters necessary to produce this data set, a modified version of LOWTRAN that accepts target reflectance and relative spectral response was used (Munechika, 1990). The data for the regression include five representative reflectance spectra from each of five broad land-cover classes; urban, soil, water, grass, and trees. These spectra were propagated through three different atmospheres: urban (5 km visibility), rural (23 km visibility), and maritime (50 km visibility).

The weighting factors determined for use are given in Table 1. It should be noted that the contribution of information by TM band 1 was very small and, because it is highly correlated with TM bands 2 and 3, was omitted for the final analysis and Equations 8 and 9 were carried out with only three independent variables, TM bands 2, 3, and 4. Similar results can be obtained by performing a no-intercept multiple linear regression with the pan band as the independent variable and the TM bands as the dependent variables; however, the global approach performed is more robust for all TM-SPOT combinations because it is based on reflectance data.

Once this synthetic panchromatic image was constructed, a linear histogram adjustment was performed to force the histogram statistics of the SPOT image to match those of the synthetic panchromatic image. This transformation of image data causes first-order atmospheric and illumination differences to be removed (Schott *et al.*, 1988). Finally, the merger was carried out on a pixel-by-pixel basis according to Equation 5, the ratio method.

TABLE 1. SUMMARY OF THE WEIGHTING FACTORS USED TO PRODUCE THE SYNTHETIC PANCHROMATIC DATA FROM THE APPROPRIATE LANDSAT TM BANDS TO MATCH THE SOT HRV PANCHROMATIC CHANNEL.

TM Band #	ω	ω(w/out TM1)
1	−0.0134	–
2	0.6417	0.5931
3	0.3175	0.3310
4	0.0311	0.0345

As a modification to this baseline method, in an attempt to define a more suitable enhancement, a check is implemented that compares each non-central pixel within a high resolution panchromatic superpixel with its neighboring superpixel center value. It is possible and likely that a pixel within a superpixel is not best represented by the ratio of multispectral to synthetic panchromatic DC. This is particularly true if a superpixel encompasses more than one spectral class (i.e., a mixed pixel). If this is the case, a provision is made that allows the ratio defined in a surrounding superpixel to be used.

A comparison scheme as shown in Figure 3 was used. The current pixel's high resolution panchromatic value was compared with the central superpixel values of its neighbors as well as the central value of the superpixel in which it was contained. If the current pixel's value was closer to one of the neighboring superpixel values, then the corresponding ratio is used in place of its own superpixel ratio. This will reduce some of the blockiness that may appear in the merged image and allows each pixel in a superpixel to be processed through a different correlation ratio, allowing for preservation of mixed spectral characteristics (e.g., mixed pixels).

Evaluation Criteria

A two-fold evaluation process was carried out in order to access the quality of the resulting merged image set. The RMS error between the merged data set and a "truth" data set was computed and the classification accuracy resulting from a standard gaussian maximum-likelihood classifier was determined.

In order to properly compute the RMS error present after the merger of the data sets, one needs a "truth" image. In order to accomplish this, a merger was carried out with two degraded image sets. A SPOT HRV PAN (10-m) image was pixel averaged over 3 by 3 neighborhoods to obtain an image with 30-m resolution. The same was done to a Landsat TM data set to obtain a 90-m GIFOV. This degradation assumes a linear radiance mixing model and has been found to be a reasonable approximation for coarser resolution sensors (Merickel *et al.*, 1984; Chhikara, 1984). Then a scene merger could be performed to create a 30-m high resolution hybrid multispectral image that can be directly compared to the original TM data set. The RMS error for each band is computed as

$$\epsilon(i) = \sqrt{\frac{\sum_{n=1}^{N} (\text{Hybrid}_i(n) - \text{TM}_i(n))^2}{N}} \tag{10}$$

where $\text{Hybrid}_i(n)$ is the nth digital count of the ith band of the merged output, $\text{TM}_i(n)$ is the original TM digital count in the ith band, and N is the total number of pixels in the image. The total RMS error is then reported as

$$\text{Total RMS error} = \epsilon(1) + \epsilon(2) + \epsilon(3) + \epsilon(4) + \epsilon(5) + \epsilon(7) \tag{11}$$

In the evaluation of classification accuracy, the original full resolution SPOT HRV PAN (10-m) and Landsat TM (30-m) data set were utilized to produce a 10-m hybrid output data set. In addition to the six reflective bands, a standard deviation image derived over 3 by 3 local neighborhoods on TM band 4 and an infrared-to-red ratio image (TM bands 5 to 3) were used as input to the gaussian maximum-likelihood classifier. Classification accuracy was then established according to two methods.

Independent data sets were selected from the image to represent the five land-cover classes desired: urban, soil, water, trees, and grass. These data sets consisted of contiguous, homogeneous groups of pixels for each land-cover type. The pixels in these groups were classified, and the resulting class was compared to the known cover type. Percentage classification accuracy was the overall average of the individual class accuracies.

A second more robust analysis of classification accuracy was carried out in which random points from each class were selected and presented to the user. The user was then tasked to identify the class to which the pixel belonged based on ground truth data, air photos, and maps. This user assigned class was taken to be truth, and the classifier assignments were compared to them. Again, the reported overall classification accuracy from this technique represents an average of the individual class accuracies. Fifty random points were selected from each land-cover type.

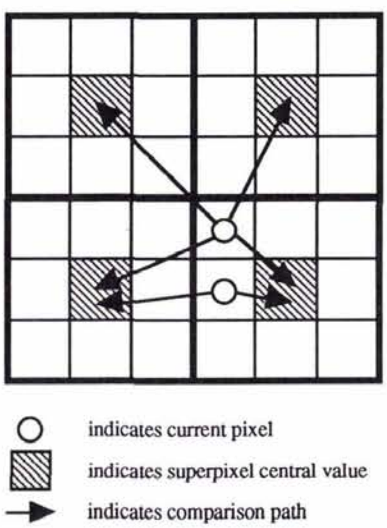

Fig. 3. Comparison scheme used for a 3 by 3 superpixel for representative positions (corner pixels are compared in four directions while side pixels are only compared in two directions).

Results

The ratio method presented in this study and its modified implementation were applied to a SPOT HRV PAN and Landsat TM data set. The images used were of a small section of Rochester, New York. The SPOT PAN image was acquired on 10 June 1987 and the Landsat TM image was acquired five days later on 15 June 1987. The sun elevation angles for these two data acquisitions were 65.9° and 59.0°, respectively. In addition to the merger methods described in this paper, Price's merger method (Price, 1987) described earlier was also implemented as a point of reference.

The original data sets are shown in Plates 1a and 1b. The results of the merger algorithms are shown in Plates 1c through 1e.

Tables 2 and 3 summarize the radiometric error incurred by these merger methods and present the improved classification accuracy attainable by using the hybrid data sets over the original multispectral data. The total RMS error (sum for six bands) in digital counts for all bands when weakly correlated bands were treated using Price's approach was 38.4, while using the simple ratio method gave an error of 48.8. This dif-

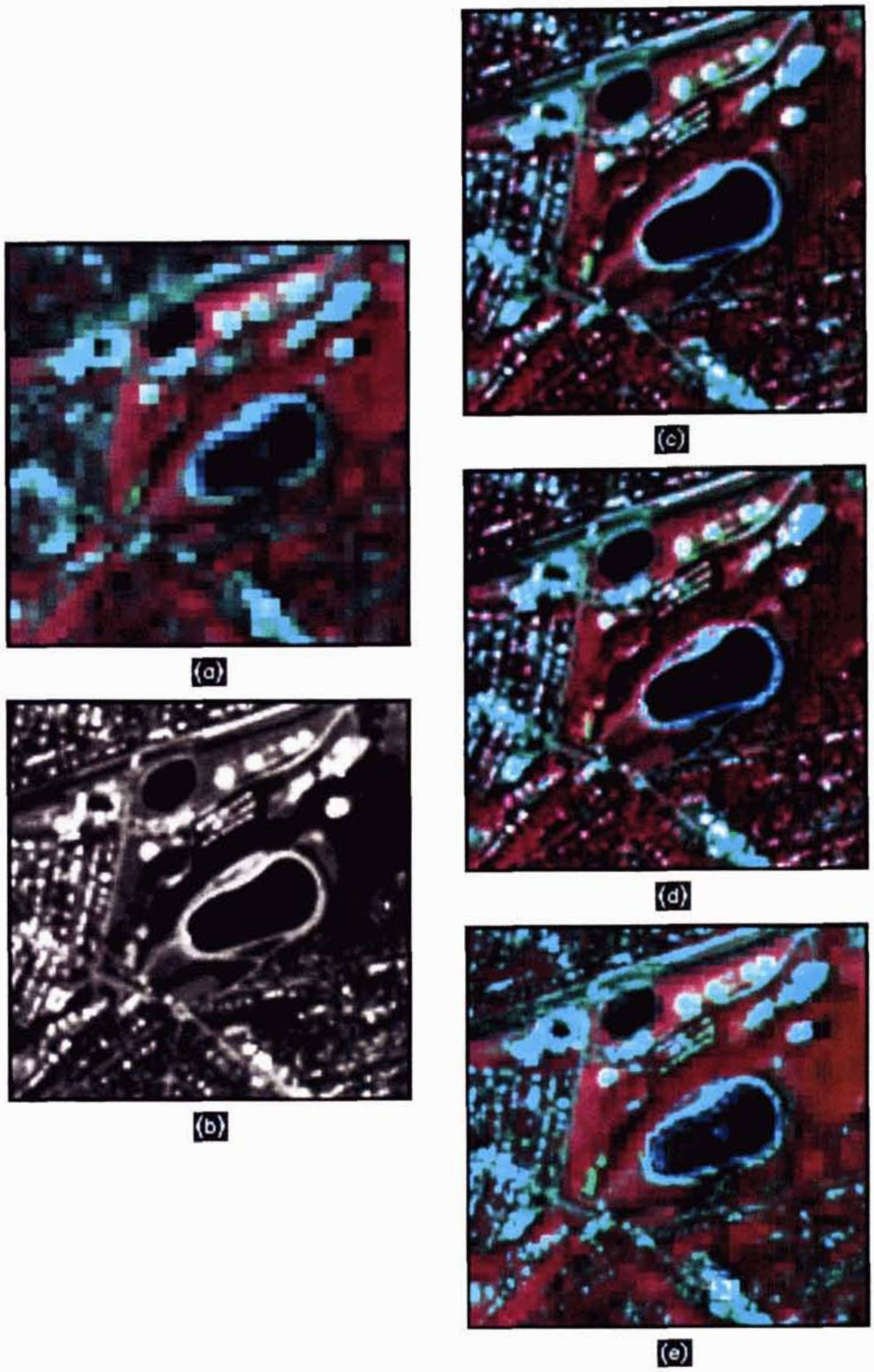

Plate 1. Merged image results: (a) original Landsat TM bands 5, 3, and 2 (R,G,B), (b) original SPOT HRV PAN, (c) merged results using the ratio enhancement method (bands 5, 3, and 2 of the hybrid data set), (d) merged results using the ratio enhancement method with the neighborhood comparison modification (bands 5, 3, and 2 of the hybrid data set), and (e) merged results using Price's merger method (Price, 1987) with LUT modification for weakly correlated bands (bands 5, 3, and 2 of the hybrid data set).

ference in RMS error, however, did not affect the improvement in classification accuracy, an average of 93.8 percent for the two methods accounting for weakly correlated bands and 95.7 percent for the simple ratio method on an independent data set.

It should be noted that applying the ratio method to all bands (even those showing weak correlation with the pan band) provided an equal improvement in classification accuracy of an independent data set to that obtained with Price's method for weakly correlated bands (95.7 percent for the ratio method compared to 95.1 percent for Price's method). The random data point analysis showed similar results with lower classification accuracies. This reduction in accuracy is due to the "pessimistic" nature of this technique. Random data point analysis assumed that the user is capable of supplying "truth" data for random points throughout the scene, a task that is not always feasible.

Conclusions

The scene merger methods presented produced image data that resulted in a statistically significant increase in classification accuracy (approximately 6 percent) when compared with land-cover maps formed from the original multispectral data set. As for radiometric accuracy, the RMS errors reported for all bands combined indicate that the three methods implemented perform very closely to each other. The maximum errors occur in those bands that do not exhibit a strong correlation with the original high resolution panchromatic data, namely, TM bands 4, 5, and 7. For those bands showing strong correlation with the original panchromatic data, RMS errors of less than 1.5 percent reflectance are obtained using any of the methods presented (converting DC units to reflectance units).

Work is currently under way to develop improved methods for dealing with weakly correlated bands. Price's method incorporated a simple attempt at this; however, the improvement in RMS error of 10 DC over the baseline ratio method presented here did not manifest itself in improved classification accuracy.

All methods provide superior visual interpretability as judged by the authors.

TABLE 2. SUMMARY OF TOTAL RMS ERROR FOR THE 30-M HYBRID IMAGE (ALL BANDS).

Enhancement Method	Band RMS error (DC)	Total RMS error (DC)
Ratio method	–	48.8
Band 1	8.26	–
Band 2	3.65	–
Band 3	5.24	–
Band 4	16.73	–
Band 5	9.93	–
Band 7	4.98	–
Ratio (checking neighbors)	–	40.7
Band 1	6.14	–
Band 2	2.61	–
Band 3	4.11	–
Band 4	14.92	–
Band 5	8.71	–
Band 7	4.20	–
Price's method (w/LUT)	–	38.4
Band 1	5.22	–
Band 2	2.78	–
Band 3	4.95	–
Band 4	12.24	–
Band 5	8.22	–
Band 7	5.04	–

TABLE 3. SUMMARY OF CLASSIFICATION ACCURACY WITH RANDOM DATA POINT SELECTION AND INDEPENDENT DATA SET FOR THE 10-M HYBRID IMAGE.

Enhancement Method	Random data point analysis	Independent data set (overall)
Original TM (30m)	74.2%	83.2%
Ratio method	80.8%	95.7%
Ratio (checking neighbors)	80.8%	92.4%
Price's method (w/LUT)	79.6%	95.1%

References

Chavez, P. S., G. L. Berlin, and M. A. Tarabzouni, 1983. Discriminating lithologies and surficial deposits in the AL Hisma plateau region of Saudi Arabia with digitally combined Landsat MSS and SIR-A images: *Proceedings of the National Conference on Resource Management Applications: Energy and Environment*, Vol. 4, San Francisco, California, pp. 22–34.

Chavez, P. S., S. C. Sides, and J. A. Anderson, 1991. Comparison of three different methods to merge multiresolution and multispectral data: Landsat TM and SPOT Panchromatic: *Photogrammetric Engineering & Remote Sensing*, Vol. 57, No. 3, pp. 295–303.

Chhikara, R. S., 1984. Effects of mixed (boundary) pixels on crop proportion estimation: *Remote Sensing of Environment*, Vol. 14, pp. 207–218.

Daily, M., T. Farr, C. Elachi, and G. Schaber, 1979. Geologic interpretation from composited radar and Landsat imagery: *Photogrammetric Engineering & Remote Sensing*, Vol. 45. No. 8, pp. 1109–1116.

Kneizys, F. X., E. P. Shettle, L. W. Abreu, J. H. Chetwynd, G. P. Anderson, W. O. Gallery, J. E. A. Selby, and S. A. Clough, 1988. *Users Guide to LOWTRAN 7*. Air Force Geophysics Laboratory, Optical/Infrared Technology Division, Hanscom AFB, Mass.

Lauer, D. T., and W. J. Todd, 1981. Land cover mapping with merged Landsat RBV and MSS stereoscopic images: *Proceedings of the ASP Fall Technical Conference*, American Society for Photogrammetry, San Francisco, California, pp. 680–689.

Lillesand, T. M., and R. W. Kiefer, 1979. *Remote Sensing and Image Interpretation*, John Wiley & Sons, New York.

Merickel, M. B., J. C. Lundgren, and S. S. Shen, 1984. A spatial processing algorithm to reduce the effects of mixed pixels and increase the separability between classes: *Pattern Recognition*, Vol. 17, No. 5, pp. 525–533.

Munechika, C. K., 1990. *Merging Panchromatic and Multispectral Images for Enhanced Image Analysis:* M.S. Thesis, Rochester Institute of Technology, Rochester, New York.

Pradines, D., 1986. Improving SPOT images size and multispectral resolution: *Proceedings of the S.P.I.E. Earth Remote Sensing using the Landsat Thematic Mapper and SPOT Systems*, Vol. 660, pp. 98–102.

Price, J. C., 1987. Combining panchromatic and multispectral imagery from dual resolution satellite instruments: *Remote Sensing of Environment*, Vol. 21, pp. 119–128.

Schott, J. R., C. Salvaggio, and W. J. Volchok, 1988. Radiometric scene normalization using pseudoinvariant features: *Remote Sensing of Environment*, Vol. 26, No. 1, pp. 1–16.

Schowengerdt, R. A., 1982. Enhanced thermal mapping with Landsat and HCMM digital data: *Technical Papers from ACSM-ASP Convention, 48th Annual Meeting*, American Society of Photogrammetry, Denver, Colorado, pp. 414–422.

Suits, G., W. Malila, and T. Weller, 1988. Procedures for using signals from one sensor as substitutes for signals of another: *Remote Sensing of Environment*, Vol. 25, No 3, pp. 395–408.

(Received 12 August 1991; revised and accepted 3 June 1992)